Entangled-state generation and Bell inequality violations in nanomechanical resonators

J. Robert Johansson,[1] Neill Lambert,[2] Imran Mahboob,[3] Hiroshi Yamaguchi,[3] and Franco Nori[2,4]
[1]*iTHES Research Group, RIKEN, Saitama 351-0198, Japan*
[2]*CEMS, RIKEN, Saitama 351-0198, Japan*
[3]*NTT Basic Research Laboratories, Nippon Telegraph and Telephone Corporation, Atsugi 243-0198, Japan*
[4]*Physics Department, University of Michigan, Ann Arbor, Michigan 48109, USA*
(Received 4 March 2014; revised manuscript received 7 November 2014; published 24 November 2014)

We investigate theoretically the conditions under which a multimode nanomechanical resonator, operated as a purely mechanical parametric oscillator, can be driven into highly nonclassical states. We find that when the device can be cooled to near its ground state, and certain mode matching conditions are satisfied, it is possible to prepare distinct resonator modes in quantum entangled states that violate Bell inequalities with homodyne quadrature measurements. We analyze the parameter regimes for such Bell inequality violations, and while experimentally challenging, we believe that the realization of such states lies within reach. This is a re-imagining of a quintessential quantum optics experiment by using phonons that represent tangible mechanical vibrations.

DOI: 10.1103/PhysRevB.90.174307 PACS number(s): 85.85.+j, 05.45.−a, 03.65.Ud

I. INTRODUCTION

Reaching the quantum regime with mechanical resonators have been a long-standing goal in the field of nanomechanics [1–4]. In recent experiments, such devices have been successfully cooled down to near their quantum ground states [5–7], and in the future may be used for quantum metrology [8], as quantum transducers and couplers between hybrid quantum systems [9–15], for quantum information processing [16], and for exploring the limits of quantum mechanics with macroscopic objects. In many of these applications it is essential to both prepare the nanomechanical system in highly nonclassical states and to unambiguously demonstrate the quantum nature of the produced states.

Nonclassical states of harmonic resonators can be achieved by introducing time-dependent parametric modulation [17] or via nonlinearities. The latter can be realized by a variety of techniques, for example by coupling to a superconducting qubit [5], coupling to additional optical cavity modes [18–21], applying external nonlinear potentials [16], or via intrinsic mechanical nonlinearities in the resonator itself [22–25]. Using such nonlinearities, specific modes of a nanomechanical resonator could potentially be prepared in a rich variety of different nonclassical states, such as quadrature squeezed states [18,26–30], sub-Poissonian phonon distributions [31–33], Fock states [34], and quantum superposition states [5,35,36]. Quantum correlations and entanglement between states of distinct oscillator modes could also be potentially generated, typically taking the form of entangled phonon states and two-mode quadrature correlations and squeezing [37–40]. Experimentally, nonlinear interactions between modes of nanomechanical resonators have already been used [41,42] for parametric amplification and noise squeezing. Various schemes [34,43,44] have proposed using nonlinear dissipation processes to realize steady state entanglement. In a similar direction, a recent proposal [45] looked at ways to couple different internal mechanical modes of a nanomechanical system via ancillary optical cavities. Also, Rips *et al.* [34] looked at ways to prepare nonclassical states using enhanced intrinsic mechanical nonlinearities.

Here we consider the generation of nonclassical states and the subsequent violation of Bell inequalities by the use of similar intrinsic mechanical nonlinearities [16,23–25]. We focus on a model relevant to a recent experimental realization [46] of a phonon laser, where a single mechanical device exhibits significant coupling between three internal modes of deformation, due to asymmetries in the beam [25], and selective activation using external driving. Here we examine that same intrinsic intermode interaction in the quantum limit. A schematic illustration of the device considered here is shown in Fig. 1, though this is not intended to be representative of the ideal realization or measurement scheme for operating in the quantum limit. In most of our discussion we do not consider an explicit physical setup but rather focus on setting bounds on the fundamental system parameters necessary to realize the phenomena we discuss. The model we derive consists of an adiabatically eliminated pump mode which drives the interaction between two lower-frequency signal and idler modes. We show that in the transient regime one can obtain violations of a Bell inequality based on correlations between quadrature measurements of the signal and idler modes. This is a re-imagining of a quintessential quantum optics experiment by using phonons that represent tangible mechanical vibrations.

This paper is organized as follows: In Sec. II we introduce the general model and the Hamiltonian for a nonlinear nanomechanical device. In Sec. II A we consider a regime in which a parametric oscillator is realized using three modes in the mechanical system, and in Sec. II B we introduce an effective two-mode model, valid when the pump mode can be adiabatically eliminated, and we analyze the types of nonclassical states that can be generated in this system. In Sec. III we review Bell's inequality using quadrature measurements, and in Sec. IV we analyze the conditions for realizing a violation of this quadrature-based Bell inequality with the mechanical system in the parametric oscillator regime studied in Sec. II B. Finally, we discuss the outlook for an experimental implementation using either intrinsic nonlinearities in Sec. V, or, as an alternative, optomechanical nonlinearities in Sec. V C. We summarize our results in Sec. VII.

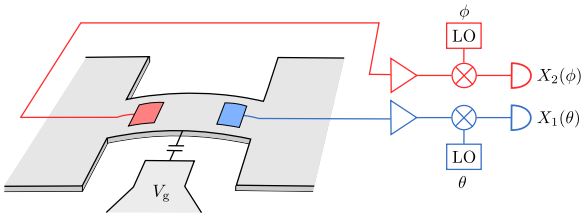

FIG. 1. (Color online) Schematic illustration of a conceptual nanomechanical resonator with two homodyne measurement setups that probe two different modes of oscillation. The beam can oscillate in a large number of vibrational and flexural modes with different frequencies. The two homodyne detectors measure the mode quadratures $X_1(\phi)$ and $X_2(\theta)$ with frequencies $\omega_1/2\pi$ and $\omega_2/2\pi$, respectively. By analyzing the correlations between the $X_1(\phi)$ and $X_2(\theta)$ quadratures, it is possible to determine whether or not the mode states are quantum-mechanically entangled.

II. MODEL

The general Hamiltonian for a nonlinear multimode resonator, describing both the self-nonlinearities and multimode couplings up to fourth order, can be written as [24]

$$H = \sum_k \omega_k a_k^\dagger a_k + \sum_{klm} \beta_{klm} x_k x_l x_m + \sum_{klmn} \eta_{klmn} x_k x_l x_m x_n + O(x^5), \quad (1)$$

where ω_k is the frequency, a_k is the annihilation operator, and $x_k = a_k + a_k^\dagger$ is the quadrature of the mechanical mode k. Here the basis has been chosen so that linear two-mode coupling terms are eliminated. The third-order mode-coupling tensor β_{klm} describes the odd-term self-nonlinearity and the trilinear multimode interaction. The fourth-order terms describes the even-term self-nonlinearity and fourth-order multimode coupling. In symmetric systems the fourth-order terms dominate (odd terms vanish due to symmetry), and it has been proposed elsewhere that they can be used to create effective mechanical qubits [16]. The possible combination of both third- and fourth-order terms will be briefly considered in the final section. The strength of the nonlinearity depends on the fundamental frequency (length) of the resonator, and can be enhanced by a range of techniques [16]. In this work we focus on the three-mode coupling terms, as these are necessary to generate the states that violate continuous variable Bell inequalities. Such terms vanish in symmetric systems and thus depend on the degree of asymmetry in the mechanical device [24,25], which again can be enhanced with fabrication techniques. Our approach in the following is to identify the ideal situation under which one can realize these rare Bell inequality violating states. Ultimately these states will be degraded by losses (which we investigate), but also by unwanted nonlinearities from the above Hamiltonian.

A. Parametric oscillator regime

Nanomechanical devices of the type described in the previous section have a large number of modes with different frequencies which depend on the microscopic structural properties of the beam. Here we focus on three such modes

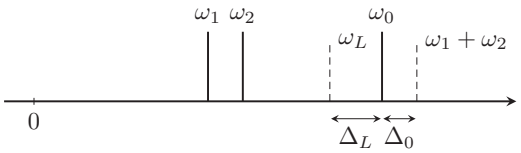

FIG. 2. A visualization of the mode-matching condition required to obtain an effective three-mode system. The modes are represented as solid vertical lines, and the driving frequency and the sum of the signal and idler frequencies, which should sum up to a frequency close to ω_0, are represented by dashed vertical lines.

(relabeled as $k = 0,1,2$) which are chosen such that they satisfy the phase-matching condition $\omega_1 + \omega_2 = \omega_0 + \Delta_0$, where $\Delta_0 \ll \omega_0$. In this case we can perform a rotating-wave approximation to single out the slowly oscillating coupling terms, and obtain the desired effective three-mode system, neglecting any higher-order nonlinearities. In the original frame, the Hamiltonian with this rotating-wave approximation is

$$H = \sum_{k=0}^{2} \omega_k a_k^\dagger a_k + i\kappa(a_1^\dagger a_2^\dagger a_0 - a_1 a_2 a_0^\dagger), \quad (2)$$

where a_1 and a_2 are the signal and idler modes, respectively, and a_0 is the pump mode. Furthermore, we apply a driving force that is nearly resonant with ω_0, with frequency $\omega_L = \omega_0 - \Delta_L$, $|\Delta_L| \ll \omega_0$, and transform the above Hamiltonian to the rotating frame where the resonant drive terms are time independent,

$$H = \Delta_L a_0^\dagger a_0 + \sum_{k=1,2} \Delta_k a_k^\dagger a_k + i\kappa(a_1^\dagger a_2^\dagger a_0 - a_1 a_2 a_0^\dagger) - i(E a_0^\dagger - E^* a_0). \quad (3)$$

Here $\Delta_1 = \Delta_2 = (\Delta_0 - \Delta_L)/2$, $\kappa = \beta_{012}$ is the intermode interaction strength, and E is the driving amplitude of mode a_0. See Fig. 2 for a visual representation of the mode-matching condition and the detuning parameters Δ_0 and Δ_L.

This is an all-mechanical realization of the general three-mode parametric oscillator model in nonlinear optics [47,48], where mode a_0 is the quantized pump mode, and modes a_1 and a_2 are the signal and idler modes, respectively.

B. Effective two-mode model

We assume that in this purely nanomechanical realization of the parametric oscillator model, Eq. (3), all three mechanical modes interact with independent environments. We describe these processes with a standard Lindblad master equation on the form

$$\dot{\rho} = -i[H,\rho] + \sum_k \gamma_k\{(N_k + 1)\mathcal{D}[a_k] + N_k \mathcal{D}[a_k^\dagger]\}\rho, \quad (4)$$

where $\mathcal{D}[a_k]\rho = a_k \rho a_k^\dagger - \frac{1}{2} a_k^\dagger a_k \rho - \frac{1}{2}\rho a_k^\dagger a_k$ is the dissipator of mode a_k, γ_k is the corresponding dissipation rate, and the average thermal occupation number is $N_k = [\exp(\hbar\omega_k\beta) - 1]^{-1}$. Here $\beta = 1/k_B T$ is the inverse temperature T, and k_B is Boltzmann's constant.

Assuming that the pump mode is strongly damped compared to the signal and idler modes, $\gamma_0 \gg \gamma_1, \gamma_2$, and that

the pump-mode dissipation dominates over the coherent interaction, $\gamma_0 \gg \langle H \rangle \sim \kappa \langle a_0^\dagger a_1 a_2 \rangle$, one can adiabatically eliminate [48,50,51] the pump mode from the master equation given above. Here we also assume that the high-frequency pump mode is at zero temperature, $N_0 = 0$, while the temperatures of modes a_1 and a_2 can remain finite. This results in a two-mode master equation that includes correlated two-phonon dissipation, where one phonon from each mode dissipates to the environment through the pump mode, in addition to the original single-phonon losses in each mode:

$$\dot{\rho} = -i[H',\rho] + \gamma \mathcal{D}[a_1 a_2]\rho + \sum_{k=1,2} \gamma_k \{(N_k+1)\mathcal{D}[a_k] + N_k \mathcal{D}[a_k^\dagger]\}\rho, \quad (5)$$

where the effective two-phonon dissipation rate is

$$\gamma = \frac{\kappa^2 \gamma_0/2}{|\gamma_0/2 + i\Delta_L|^2}. \quad (6)$$

The reduced two-mode Hamiltonian is given by

$$H' = \sum_{k=1,2} \Delta_k a_k^\dagger a_k + i(\mu a_1^\dagger a_2^\dagger - \mu^* a_1 a_2) + \chi a_1^\dagger a_1 a_2^\dagger a_2, \quad (7)$$

with the two-mode interaction strength

$$\mu = \frac{E\kappa}{\gamma_0/2 + i\Delta_L}, \quad (8)$$

and the effective cross-Kerr interaction strength

$$\chi = -\frac{\kappa^2 \Delta_L}{|\gamma_0/2 + i\Delta_L|^2}, \quad (9)$$

which vanishes when the driving field is at exact resonance with the pump mode. In the following we will generally assume that this resonance condition can be reached, and Δ_L will be set to zero in the equations above.

In this resonant limit the Hamiltonian H' describes an ideal two-mode parametric amplifier, which is well known to be the generator of two-mode squeezed states [52]. When applied to the vacuum state, or a low-temperature thermal state, the resulting two-mode squeezed states are nonclassically correlated [53], but when viewed individually, both modes appear to be in thermal states. In spite of being quantum mechanically entangled, these two-mode squeezed states have a positive Wigner function and cannot violate the quadrature binning Bell inequalities [54] that we consider below. One must consider the effect of the two-phonon dissipation in Eq. (5) to induce such violations.

In the highly idealized case when single phonon dissipation in the a_1 and a_2 modes is absent, i.e., $\gamma_1 = \gamma_2 = 0$, but with $\gamma_0 > 0$, the model Eq. (5) produces a steady state [50] of the form

$$\rho = \frac{1}{I_0(2r^2)} \sum_{m,n} \frac{r^{2m+2n}}{m!n!} |m,m\rangle\langle n,n|, \quad (10)$$

where I_0 is the zeroth order modified Bessel function and $r = \sqrt{2E/\kappa}$. The special structure of this steady state, with equal number of phonons in each mode, is because both the Hamiltonian and two-phonon dissipator conserve the phonon-number difference $a_2^\dagger a_2 - a_1^\dagger a_1$. However, this symmetry is broken if the single-phonon dissipation processes are included in the model, i.e., $\gamma_1, \gamma_2 > 0$. The state Eq. (10) is visualized in Fig. 3 for the specific set of parameters given in the figure caption. Figures 3(a) and 3(b) show the Fock-state distribution and the Wigner function for the modes a_1 and a_2 (because of symmetry the states of both modes are identical in this case, and only one is shown). In this case the states of the two modes no longer appear to be thermal when viewed individually, but the reduced single-mode Wigner functions are positive and thus, on their own, each mode appears classical. However, together the two-mode Wigner function can be negative. For example, there is a strong cross-quadrature correlation, as shown in Fig. 3(c). The variances of the cross-quadrature differences, in the transient approach to the steady state, are shown in Fig. 4, and exactly in the steady state the variance of the squeezed two-mode operator difference is

$$\mathrm{Var}(x_1 - x_2) = 1 + 2r^2 \frac{I_1(2r^2)}{I_0(2r^2)} - 2r^2, \quad (11)$$

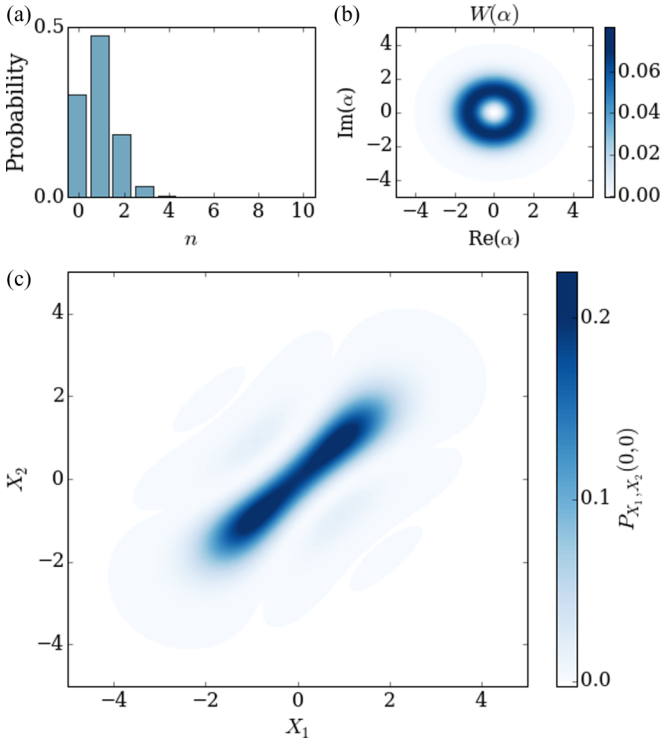

FIG. 3. (Color online) Visualization of the steady state of the effective two-mode system. (a) The Fock state distribution of modes a_1 and a_2. (b) The single-mode Wigner function of modes a_1 and a_2. Both the Fock state distribution and the Wigner function are identical for both modes a_1 and a_2, due to the symmetric two-phonon processes and equal dissipation rates and initial states. The single-mode Wigner function is positive, and the single-mode state can therefore be considered classical. However, strong correlations exists between quadratures of two different modes, as shown in the joint quadrature probability distribution $P_{X_1,X_2}(0,0)$ in (c). Here we have used the parameters $\kappa = 0.15$, $E = 0.094$, $\gamma_0 = 1.0$, $\gamma_1 = \gamma_2 = 0$, and $\Delta_0 = \Delta_L = 0$. These parameters were chosen to produce a steady state that closely corresponds to the ideal state [49] for quadrature Bell inequality violation, i.e., with $r = 1.12$ (see Sec. IV A).

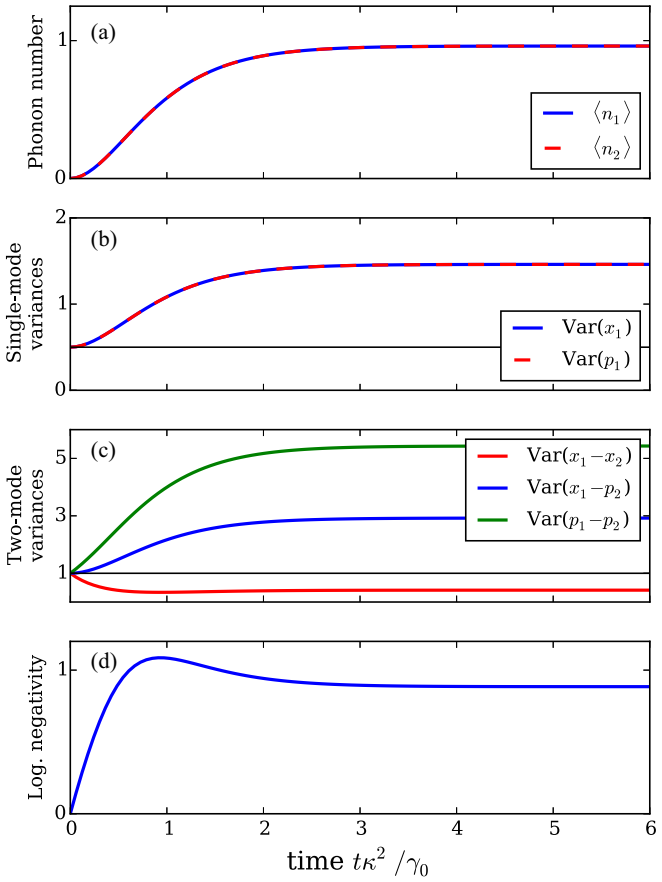

FIG. 4. (Color online) The time evolution of the phonon number (a), single-mode quadrature variances (b), and the variances of the two-mode quadrature differences (c), the logarithmic negativity (d), for the case when the state is initially in the zero-temperature ground state. In the large-time limit the state approaches the steady state that is visualized in Fig. 3. The single-mode variances increase above the vacuum limit as time increases, but the variance of cross-quadrature difference $\mathrm{Var}(x_1 - x_2)$ decrease below the vacuum limit, which is a characteristic of two-mode squeezing, and the nonzero logarithmic negativity demonstrates that the steady state is nonclassical. Here we used the same parameters as those given in the caption of Fig. 3.

which in the limit of large r approaches $1/2$, but has a local minimum of about 0.4 at $r \approx 0.92$. We note that for the vacuum state $\mathrm{Var}(x_1 - x_2) = 1$, and thus this quadrature difference variance is therefore squeezed below the vacuum level for any $r > 0$. The logarithmic negativity [55] shown in Fig. 4(d) further demonstrates the nonclassical nature of this state.

These intermode quadrature correlations, with squeezing below the vacuum level of fluctuations, are nonclassical and it has been shown that this particular state can violate Bell inequalities based on quadrature measurements [54], as we will discuss in the next section. In fact, this steady state is, for a certain value of r, a good approximation to the ideal two-mode quantum state [49] for these kinds of Bell inequalities. However, it has also been shown that in the presence of single phonon dissipation the steady state two-mode Wigner function is always positive, and thus exhibits a hidden-variables description and cannot violate any Bell inequalities [47]. Fortunately, this is only the case for the steady state, and there can be a significant transient period in which the two-mode system is in a state that can give a violation.

In the following we consider two regimes; the steady state, and the slow transient dynamics of a system that is originally in the ground state, and approaches the new steady state after the driving field has been turned on.

III. BELL INEQUALITIES FOR NANOMECHANICAL SYSTEMS

Verifying that a nanomechanical system is in the quantum regime, and that the states produced in the system are nonclassical, can be sometimes be experimentally challenging, largely because of the difficulty in implementing single-phonon detectors in nanomechanical systems. As has been done in circuit QED [56,57], measuring a nonlinear energy spectrum [16] would be a convincing indication that the system is operating in the quantum regime, although it does not imply that the state of the system is nonclassical, and all quantum nanomechanical systems need not necessarily be nonlinear. A number of techniques could be used to demonstrate that the state is nonclassical [58], for example reconstructing the Wigner function using state tomography and looking for negative values, or evaluating entanglement measures such as the logarithmic negativity (for Gaussian states) or entanglement entropy (suitable only at zero temperature).

Here we are interested in a nonclassicality test that can be evaluated using joint two-mode quadrature measurements. The two-mode squeezing shown in the previous section can be considered as an entanglement witness [59,60], and was recently investigated experimentally in an optomechanical device [28,29]. The quadrature-based Bell inequality can be seen as another, stricter, example of a nonclassicality test, and in the following we focus on the possibility of violating these Bell inequalities with the nanomechanical system outlined in the previous section. Even though one cannot rule out the locality loophole in such a system, and thus a violation would lack any meaning as a strict test of Bell nonlocality [61], it would still serve as a very satisfying test for two-mode entanglement.

The original Bell inequalities are formulated for dichotomic measurements, with two possible outcomes. However, dichotomic measurements are not normally available in harmonic systems like the nanomechanical systems considered here, where the measurement outcomes are, for the most part, continuous and unbound. In this continuous-variable limit one must choose how to perform a Bell inequality test with care. Generalized inequalities for unbound measurements exist [62], but are both extremely challenging to implement and hard to violate. Fortunately one can implement CHSH-type Bell inequality by binning quadrature measurements, and thus obtaining a dichotomic bound observable. Munro [49] showed that, while in general it is hard to generate states which can violate such an inequality, it is possible to generate precisely the type of states which do cause a violation with a nondegenerate parametric oscillator, which is analogous to the system we investigate here.

One possible binning strategy [54,63] for the continuous outcomes of quadrature measurements of the mechanical

modes is to classify the outcomes as 1 if the measurement outcome is $X_\theta > 0$, and 0 otherwise. The probability of the outcomes 0 and 1 for the two modes can then be written

$$P_{\alpha\beta}(\theta,\phi) = \int_{L(\alpha)}^{U(\alpha)} \int_{L(\beta)}^{U(\beta)} d^2X p\left(X_1^\theta, X_2^\phi\right)[\rho], \quad (12)$$

where

$$L(\alpha) = \begin{cases} 0 & \text{if } \alpha = 1 \\ -\infty & \text{if } \alpha = 0 \end{cases}, \quad U(\alpha) = \begin{cases} \infty & \text{if } \alpha = 1 \\ 0 & \text{if } \alpha = 0 \end{cases}. \quad (13)$$

Here ρ is the two-mode density matrix and $p(X_1^\theta, X_2^\phi)[\rho]$ is the probability distribution for obtaining the measurement outcomes X_1^θ and X_2^ϕ for the signal and idler mode quadratures

$$x_1^\theta = a_1 e^{-i\theta} + a_1^\dagger e^{i\theta}, \quad (14)$$

$$x_2^\phi = a_2 e^{-i\phi} + a_2^\dagger e^{i\phi}, \quad (15)$$

respectively. This probability distribution is given by

$$\begin{aligned} p\left(X_1^\theta, X_2^\phi\right)[\rho] &= \left\langle X_1^\theta, X_2^\phi \middle| \rho \middle| X_1^\theta, X_2^\phi \right\rangle \\ &= \sum_{m,n,p,q} \rho_{(m,n),(p,q)} \frac{e^{-i(m\theta+n\phi)} e^{i(p\theta+q\phi)}}{\pi\sqrt{2^{m+n+p+q} m!n!p!q!}} \\ &\quad \times e^{-X_1^2} e^{-X_2^2} H_m(X_1) H_n(X_2) H_p(X_1) H_q(X_2), \end{aligned} \quad (16)$$

where $H_n(x)$ is the Hermite polynomial of nth order, and where we have written the density matrix in the two-mode Fock basis,

$$\rho = \sum_{m,n,p,q} \rho_{(m,n),(p,q)} |m,n\rangle\langle p,q| . \quad (17)$$

The integral in Eq. (12) can be evaluated analytically [49], but in general the sum in Eq. (16) cannot.

Treating the binned quadrature measurements as dichotomic observables we can write the standard Bell's inequalities in the Clauser-Horne (CH) [64] form

$$B_{\rm CH} = \frac{P_{11}(\theta,\phi) - P_{11}(\theta,\phi') + P_{11}(\theta',\phi) + P_{11}(\theta',\phi')}{P_1(\theta') + P_1(\phi)}, \quad (18)$$

which for a classical state satisfies $|B_{\rm CH}| \leqslant 1$, and in the Clauser-Horne-Shimony-Holt (CHSH) [65] form

$$B_{\rm CHSH} = E(\theta,\phi) - E(\theta',\phi) + E(\theta,\phi') + E(\theta',\phi'), \quad (19)$$

$$E(\theta,\phi) = P_{11}(\theta,\phi) + P_{00}(\theta,\phi) - P_{10}(\theta,\phi) - P_{01}(\theta,\phi), \quad (20)$$

which for a classical state satisfies $|B_{\rm CHSH}| \leqslant 2$. Here we have also used

$$P_1(\theta) = \int_0^\infty \int_{-\infty}^\infty d^2X p\left(X_1^\theta, X_2^\phi\right)[\rho]. \quad (21)$$

Both $B_{\rm CH}$ and $B_{\rm CHSH}$ are in general functions of the four angles θ,ϕ,θ', and ϕ'. However, to reduce the number of parameters here we consider the angle parametrization $\theta = -2\varphi$, $\phi = 3\varphi$, $\theta' = 0$, and $\phi' = \varphi$, which only leaves a single free angle parameter φ. In principle, this can reduce the magnitude of violation one can observe, but as we will see this parametrization still allows violations to occur for the types of states we are interested in here. In the following we evaluate both $B_{\rm CH}$ and $B_{\rm CHSH}$ using this angle parametrization.

IV. VIOLATION OF BELL'S INEQUALITY WITH NANOMECHANICAL RESONATORS

In this section we investigate the conditions under which the states formed in the multimode nanomechanical system may violate Bell's inequality. We emphasize again that in this context we are interested in Bell's inequality as a test that can demonstrate entanglement between different mechanical modes. We begin with an analysis of the steady state for the idealized model with $\gamma_1,\gamma_2 = 0$, and then turn our attention to the transient behavior for finite γ_1 and γ_2.

A. Steady state

With $\gamma_1,\gamma_2 = 0$, the steady state is given by Eq. (10), and inserting this state in the Bell inequalities Eqs. (18) and (19) gives an expression as a function of the steady state parameter r and the angle φ that can be optimized for maximum Bell violation. The optimal value of the angle turns out to be $\varphi = \pi/4$, and the resulting equation for optimal r is

$$I_0(2r^2)\frac{dG(r)}{dr} = 4r^2 I_1(2r^2) G(r), \quad (22)$$

but the sum over Fock-state basis that comes from Eq. (16) cannot to our knowledge be evaluated in a simple analytical form, so we have

$$\begin{aligned} G(r) = \sum_n \sum_{m>n} &\frac{8(2r^2)^{n+m}\pi}{(n!m!)^2(n-m)^2} [\mathcal{F}(n,m) - \mathcal{F}(m,n)]^2 \\ &\times \{3\cos[(n-m)\varphi] - \cos[3\varphi(n-m)]\} \end{aligned} \quad (23)$$

and

$$\mathcal{F}(n,m) = \left[\Gamma\left(\frac{1}{2} - \frac{n}{2}\right)\Gamma\left(-\frac{m}{2}\right)\right]^{-1}, \quad (24)$$

as given in Ref. [49]. Solving Eq. (22) numerically gives $r_{\rm opt} \approx 1.12$, as reported in Ref. [54]. The corresponding steady state Eq. (10) for $r_{\rm opt}$ is visualized in Fig. 3. We note that for this optimal Bell violating state the mean phonon number in each mode is only $\langle n\rangle \approx 0.94$, which highlights the need to operate the system near its ground state. If fact, when $\langle n\rangle \gg 1$ no Bell inequality violation can be observed.

In our nanomechanical model this translates to an optimal driving strength $E_{\rm opt} = r_{\rm opt}^2\kappa/2$ that maximizes the Bell inequality violation for a given nonlinearity κ. This optimal driving amplitude $E_{\rm opt}$ applies to the steady state of the idealized model without single-phonon dissipation. With finite single-phonon dissipation, the steady state does not violate any of the Bell inequalities. However, as we will see in the following section, $E_{\rm opt}$ still gives a good approximation for the optimal transient violation. While these transients are harder to capture, recent experiments on optomechanical systems have shown they are in principle possible [28,29], and relevant for the alternative proposal in the final section below. How far one can go with using multiple ancilla optical or microwave

cavities to perform similar measurements on different internal modes of a single mechanical device is not yet clear.

B. Transient

Since the more realistic model, with finite single-phonon dissipation processes, does not produce a steady state that violates any of the Bell inequalities, we are led to investigate transient dynamics. Here we focus on the transient which occurs when the driving field E is turned on after the relevant modes have been cooled to their ground states. The state of the system then evolves from the ground state to the steady state that does not violate the Bell inequalities. However, if the single phonon dissipation processes are sufficiently slow there can be a significant time interval during which the state of the system does violate the Bell inequalities.

To investigate this transient dynamics we numerically evolve the effective two-mode system described by the master equation, Eq. (5), and evaluate the $B_{\rm CH}$ and $B_{\rm CHSH}$ quantities as a function of time and the angle φ. The results shown in Fig. 5 for the situations with and without signal and idler mode dissipation and at zero temperature, demonstrate that the nanomechanical system we consider can indeed be driven into a transient state that violates both types of Bell inequalities. With losses the onset of violation is proportional to γ_0/κ^2, and the time at which the violation ceases is proportional to $\gamma_1^{-1}, \gamma_2^{-1}$, so if

$$\gamma_1, \gamma_2 \ll \kappa^2/\gamma_0, \tag{25}$$

we expect a significant period of time during the transient where the inequalities will be violated. We note that in Fig. 5(a) the regions of violation for the CH and CHSH inequalities are identical, and this is, according to our observations, always the case for this model and angle parametrization. Because of this, in the following we only show the results for the CHSH inequality.

To further explore the parameter space that can produce a Bell-inequality violation we evolve the master equation as a function of time and the parameters E, κ, and γ_0, for both the ideal case with dissipation-less signal and idler modes $\gamma_1 = \gamma_2 = 0$, and for the case including signal and idler mode dissipation $\gamma_1, \gamma_2 > 0$. In these simulations the initial state is always the ground state, and we take the temperature of the signal and idler modes to be zero. The results are shown in Figs. 6(a)–6(c) and 6(e) and 6(f), respectively. From Fig. 6 it is clear that for the case $\gamma_1 = \gamma_2 = 0$ there exist optimal values of κ and E, given that other parameters are fixed, that produce steady states that maximally violates the Bell inequality (marked with dashed lines in the figures). However, importantly we also note that the optimal values for κ and E for the steady state of the ideal model also give a good indicator for the optimal regime for the Bell violation in the transient of the case with finite single-phonon dissipation, when additionally taking into account the time scales for the transient given in Eq. (25).

When the signal and idler modes have finite temperature the region of Bell inequality violation is further reduced, as shown in Fig. 7. The detrimental effects of thermal phonons are twofold: It reduces the transient time interval during which a violation can be observed, and the nonlinear interaction

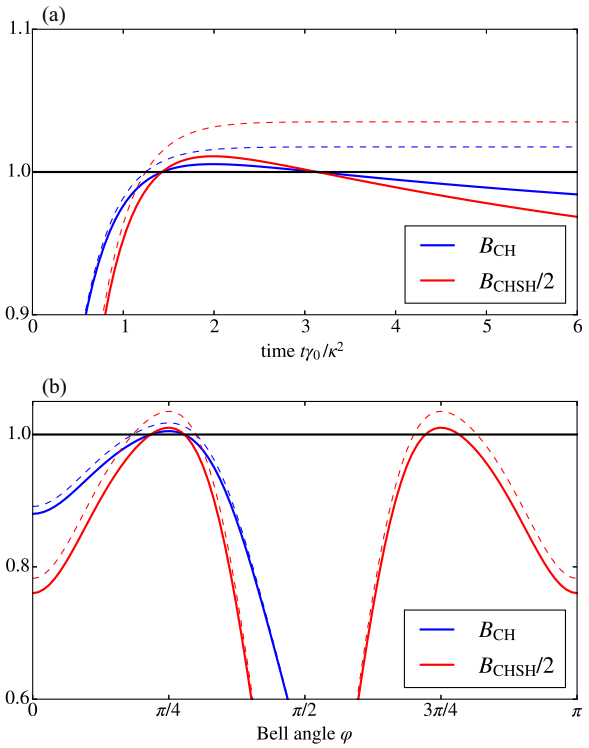

FIG. 5. (Color online) (a) The normalized CH and CHSH Bell quantities (violation above 1) as a function of time, for the pumped two-mode nanomechanical resonator, under the ideal condition without signal and idler mode dissipation (dashed line) and for the case including signal and idler dissipation. The initial state is the vacuum state, which we assume can be prepared to a good approximation using cooling. At $t = 0$, the parametric amplification is turned on by the activation of the driving field with amplitude E. In the ideal case, the steady state violates both the CH and CHSH Bell inequalities, but there is no steady state violation when single-phonon dissipation is included. However, there is a period of time during the transient where both inequalities are violated. (b) The angle φ dependence for the normalized CH and CHSH Bell quantities for $t\kappa^2/\gamma_0 = 1.8$, where solid lines include dissipation and dashed lines are the ideal case. The optimal value of φ for the states produced in the model we investigate here is $\varphi = \pi/4$, which was used in (a). The parameters used here are the same as in Fig. 3, and for the solid lines we used $\gamma_1 = \gamma_2 = 0.001$.

strength required to be able to see any violation at all increases. In fact, to observe a transient Bell inequality violation, the average thermal occupation number must be very small: An average thermal occupation number of even 0.1 phonon in the signal and idler mode is sufficient to inhibit any Bell violation with the system we have considered here. Excellent ground state cooling is therefore a prerequisite to violating a Bell inequality tests in a nanomechanical resonator.

V. EXPERIMENTAL OUTLOOK

As can be seen in Figs. 6 and 7, the violation of a Bell inequality in the system we consider here requires, as expected, a combination of low temperature, large nonlinearity, and transient quadrature measurements. These conditions can all be rather challenging to satisfy in an experimental system, but

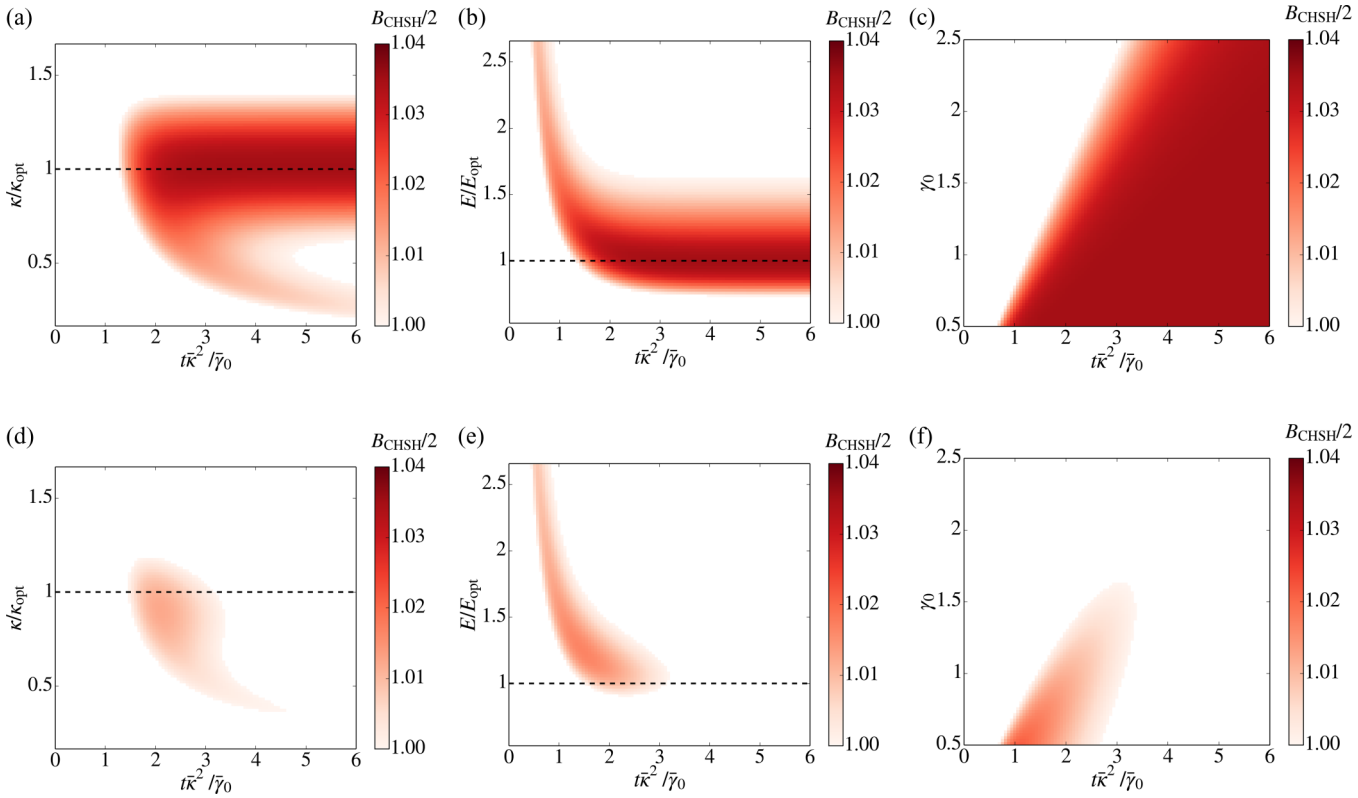

FIG. 6. (Color online) Violation of the normalized quadrature CHSH Bell inequality (redish region) as a function of time t and the intermode coupling κ (a) and (d), the pump mode driving amplitude E (b) and (e), and the pump-mode dissipation rate γ_0 (c) and (f). The ideal case without signal and idler mode dissipation is shown in (a)–(c), and (d)–(f) include signal and idler mode dissipation with equal dissipation rates $\gamma_1 = \gamma_2 = 0.001$. In (a)–(c) there is a parameter window for κ and E which results in a violation for sufficiently large t, as well as in the steady state. However, in (d)–(f) there is no violation in the steady state, but during a transient time a violation may still occur for suitably chosen parameters. Apart from the parameters on the vertical axes, the parameters were kept fixed at the same values as given in Fig. 3, and denoted by a bar over the symbol in the axes.

on the other hand they are exactly the type of conditions that one can expect would have to be satisfied for realistic quantum mechanical applications in these devices. The Bell inequality violation can therefore be seen as a benchmark that indicates that entangled quantum states can be generated and detected with high precision.

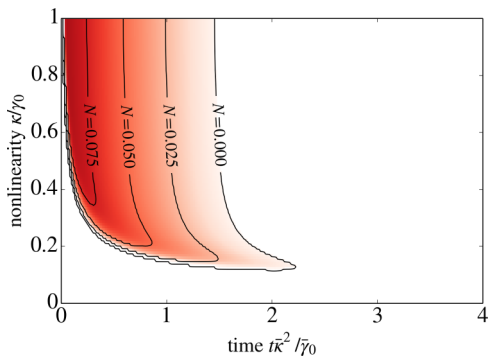

FIG. 7. (Color online) The regions where a transient Bell inequality violation can be achieved, as a function of nonlinearity κ and time t, and for different temperatures. The region of violation at zero temperature is shown in redish color. The contours mark the regions of violation for finite signal and idler mode temperatures (assumed equal), labeled by the average number N of thermal phonons. We note that even a very small number of initial thermal phonons inhibits the Bell inequality violation, which suggest that excellent ground-state cooling of both modes is a prerequisite to obtaining a violation.

A. Nonlinear interaction strength

Our proposal requires that two conditions must be met: low temperature ($k_B T \ll \hbar\omega$), and large nonlinearity with respect to dissipation in the lower modes ($\kappa^2 > \gamma_0\gamma_{1,2}$, while $\gamma_0 > \gamma_{1,2},\kappa$). The latter means we must be in what amounts to the strong-coupling limit for the interaction between the modes. While large nonlinearity and (effective) lower temperatures [5–7,66] typically require higher frequency, and thus smaller mechanical systems, the converse is true of the dissipation condition; in high frequency systems dissipation tends to increase. Experiments [22–25,67,68] involving intrinsic nonlinearities have so far only realized very weak mode-mode couplings at high temperatures. A beam-theory analysis [23] suggests that such nonlinearities increase drastically as devices are decreased in size, however there has been very little experimental investigation of such effects in smaller high-frequency devices.

One particularly relevant experiment by Castellanos-Gomez *et al.* [69] showed that nonlinear mode-mode coupling within a carbon nanotube was mediated by single-electron transport through the device (as it operates as a quantum dot

as well as a mechanical oscillator), and with this mediation they obtained a coupling strength six times larger than the intrinsic one. While this is still too small for our needs (effectively just giving $\kappa = 12$ Hz for coupling between ground states in both modes, while the loss rate of the modes in the nanotube are of the order >10 kHz) the authors also predict that the strong-coupling regime "may be reached in devices with larger Q factors and sharper Coulomb peaks" [69].

In addition, there are several other methods by which three-mode interactions may be engineered and our approach may be realized [70,71], or by which the intrinsic nonlinearity per phonon may be enhanced [16]. So far such studies have only considered two-mode interactions, but an extension to three-mode couplings is an interesting open theoretical problem.

B. Transient quadrature measurements

Performing efficient transient quadrature measurements on selected modes of the mechanical resonator is another experimental challenge. There are several levels of complexity with respect to this type of measurement: First, the mechanical motion must be converted to an electrical signal that can be detected by the measurement device. Second, the transient nature of the measurements is inherently more complex than measurements in the steady state, since it requires many cycles of the protocol (state preparation, evolution, measurement), rather than consecutive measurements in the steady state. Third, to compensate for the noise added in the amplification process, it is required to average a large number of measurements. Since the amplification of the two distinct modes adds independent Gaussian noise to each mode, it can be suppressed with sufficient averaging. However, averaging cannot eliminate systematic errors in the measurement process, such as for example detector inefficiency. Thus, finally, there is a requirement on the acceptable levels of systematic errors.

The displacement of the nanomechanical resonator can be converted to an electrical signal using a range of different techniques. For example, experiments have already demonstrated applications of piezoelectric schemes [72], coupling to a quantum-point contact [73], coupling to auxiliary optical modes [13,74], and capacitive coupling to a microwave circuit [8]. The electromechanical transduction is therefore quite well developed, and should not be a limiting factor for implementing the measurements considered here. Also, in recent experiments, transient quadrature measurements of a nanomechanical system were carried out with high precision and level of control [28,29]. Those experiments demonstrated transient quadrature measurements that are very similar to the ones required here. Thus, although challenging and potentially time consuming, transient quadrature measurements should not in principle represent any experimental problems.

The weak electrical signal from the electromechanical transduction must be amplified in order to be detectable by standard microwave measurements devices. With phase-insensitive amplification, this processes adds noise to the signal [75], which must be compensated for by averaging a large number of measurements. With extensive averaging of linearly amplified microwave fields, quadrature resolved detection of single-excitation coherent states have been demonstrated [28]. Also, in microwave electronics, quadrature measurements in the quantum regime have been applied to measure two-mode squeezing [76,77], state tomography [78], and entanglement [79]. In the Bell-inequality measurements considered here, optimal violation is expected for resonator states that correspond to about one excitation (see Fig. 3) per mode. The level of amplification and averaging to detect this weak signal is therefore similar to experimentally demonstrated measurements. Additionally, since the relative violation of the Bell inequality is about 1%–2% (see Fig. 5), we require averaging until the reconstructed quadrature correlation distribution [Eq. (16)] is consistent with a variance of B_{CHSH} [Eq. (19)] that is smaller than this relative violation. In the absence of systematic errors in the quadrature measurements, we can expect to reach this regime with sufficient averaging. However, since systematic errors, such as quadrature detection inefficiency, cannot be reduced by averaging, the maximum relative violation of the quadrature-based Bell inequality sets a fundamental limit on the acceptable systematic error in the quadrature measurement processes. However, near-quantum-limited detection of mechanical motion via microwave measurements have been demonstrated [28], and further progress in this field can be expected.

Given these recent advances in nanomechanical and microwave quadrature measurement, the outlook for realizing the required measurements for evaluating the quadrature Bell inequality is encouraging, although satisfying all the above-mentioned conditions in a single setup remains a demanding task for experimentalists.

C. Optomechanical realization

As an alternative to the purely mechanical approach discussed so far, one could observe the similar quadrature-based Bell inequality violations in an optomechanical setup akin to that proposed in Refs. [19] and [80], where a single mechanical mode is coupled to two optical cavities [81,82], e.g., in a membrane-in-the-middle geometry or within a photonic crystal cavity. The most straightforward implementation would be to use the mechanical mode as the pump mode which then acts to entangle the optical modes. The optical modes are coupled due to photon tunneling, and the resulting hybridized modes replace the mechanical signal and idler modes a_1 and a_2 discussed in this work. On resonance, this again leads to the same interaction we use in Eq. (2). The main motivation of inducing this interaction in these earlier works was to engineer anharmonic energy levels. This anharmonicity allows specific transitions to be addressed with external laser fields allowing one to use such devices as single-phonon/photon transistors and for nondemolition measurements of phonons or photons. In the limit where the mechanical pump mode can be driven and adiabatically eliminated, one in principle could observe Bell-inequality violations in the (hybridized) quadrature measurements of the two optical cavities.

VI. COMBINING EVEN AND ODD NONLINEARITIES: COUPLING MECHANICAL QUBITS

In the previous calculations we have been exclusively considering the effect of odd nonlinearities which can only

arise in asymmetric mechanical systems. In purely symmetric devices the even order terms dominate, arguably the most important of which is the x^4 Duffing nonlinearity. Recent works [16] have examined how this induces an anharmonic energy spectrum in the fundamental mode of a nanomechanical system, and outlined how this anharmonic spectrum can be used as an effective qubit for quantum computation. Naturally one can consider the effect of both the third order coupling we have outlined here, and the third and fourth order Duffing self-anharmonicity. Ultimately the relative strengths of these different terms depend strongly on the overlap between the different mode shapes within the device, the geometry of the device, and the effect of various nonlinearity enhancing mechanisms. A naive investigation of the contributions from these quartic terms suggest they only work to degrade the Bell inequality violation we discuss here. However, going beyond the regime we have outlined thus far, one may note that by changing the frequency of the driving field in Eq. (1) one can get an excitation-preserving beam-splitter type of interaction between the signal and idler modes:

$$H_{\rm int} = \mu(a_1^\dagger a_2 + a_2^\dagger a_1). \tag{26}$$

If this is combined with a sufficiently strong third- or fourth-order self-nonlinearity, such that the lowest lying energy states of each mode can be considered as a two-level system, one has a means to couple different mechanical qubits in a single device. It may be possible to construct similar interactions with ancilla cavities and optomechanical interactions [19,45]. The original parametric interaction described in Eq. (3) is not useful for this purpose as it takes one out of a single excitation subspace, as does the two-phonon dissipation.

VII. CONCLUSIONS

We have investigated a regime of a multimode nanomechanical resonator, with intrinsic nonlinear mode coupling, in which three selected modes realize a parametric oscillator. In the regime where the pump mode of the parametric oscillator can be adiabatically eliminated, we have investigated the generation of entangled states between two distinct modes of oscillation in the nanomechanical resonator, and the possibility of detecting this entanglement using quadrature-based Bell inequality tests. Our results demonstrate that while realistically it will not be possible to violate any Bell inequality in the steady state, there can be a significant duration of time in which the transient evolution from the ground state (prepared by cooling) to the steady state where the state of the system violates Bell inequalities. However, to achieve this transient violation requires a relatively large nonlinear mode coupling, excellent ground state cooling, and fast and efficient quadrature measurements. These are, of course, very challenging experimental requirements, but we believe that if a quadrature Bell inequality violation is realized experimentally it would be a very strong demonstration of quantum entanglement in a macroscopic mechanical system.

ACKNOWLEDGMENTS

The numerical simulations were carried out using QuTiP [83,84], and the source code for the simulations are available in Ref. [85]. We acknowledge W. Munro and T. Brandes for discussions and feedback. This work was partly supported by the RIKEN iTHES Project, MURI Center for Dynamic Magneto-Optics, JSPS-RFBR No. 12-02-92100, Grant-in-Aid for Scientific Research (S), and JSPS KAKENHI Grant No. 23241046.

[1] A. Cleland, *Foundations of Nanomechanics*, Advanced Texts in Physics (Springer, Berlin, 2002).
[2] M. Blencowe, Phys. Rep. **395**, 159 (2004).
[3] M. Poot and H. S. van der Zant, Phys. Rep. **511**, 273 (2012).
[4] M. Aspelmeyer, T. J. Kippenberg, and F. Marquardt, arXiv:1303.0733.
[5] A. D. O'Connell, M. Hofheinz, M. Ansmann, R. C. Bialczak, M. Lenander, E. Lucero, M. Neeley, D. Sank, H. Wang, M. Weides *et al.*, Nature (London) **464**, 697 (2010).
[6] J. D. Teufel, T. Donner, D. Li, J. W. Harlow, M. S. Allman, K. Cicak, A. J. Sirois, J. D. Whittaker, K. W. Lehnert, and R. W. Simmonds, Nature (London) **475**, 359 (2011).
[7] J. Chan, T. P. M. Alegre, A. H. Safavi-Naeini, J. T. Hill, A. Krause, S. Groblacher, M. Aspelmeyer, and O. Painter, Nature (London) **478**, 89 (2011).
[8] C. A. Regal, J. D. Teufel, and K. W. Lehnert, Nat. Phys. **4**, 555 (2008).
[9] C. P. Sun, L. F. Wei, Y.-x. Liu, and F. Nori, Phys. Rev. A **73**, 022318 (2006).
[10] M. Wallquist, K. Hammerer, P. Rabl, M. Lukin, and P. Zoller, Phys. Scr. **2009**, 014001 (2009).
[11] A. H. Safavi-Naeini and O. Painter, New J. Phys. **13**, 013017 (2011).
[12] Z.-L. Xiang, S. Ashhab, J. Q. You, and F. Nori, Rev. Mod. Phys. **85**, 623 (2013).
[13] J. Bochmann, A. Vainsencher, D. D. Awschalom, and A. N. Cleland, Nat. Phys. **9**, 712 (2013).
[14] T. Bagci, A. Simonsen, S. Schmid, L. G. Villanueva, E. Zeuthen, J. Appel, J. M. Taylor, A. Sorensen, K. Usami, A. Schliesser *et al.*, Nature (London) **507**, 81 (2014).
[15] R. W. Andrews, R. W. Peterson, T. P. Purdy, K. Cicak, R. W. Simmonds, C. A. Regal, and K. W. Lehnert, Nat. Phys. **10**, 321 (2014).
[16] S. Rips and M. J. Hartmann, Phys. Rev. Lett. **110**, 120503 (2013).
[17] L. Tian, M. S. Allman, and R. W. Simmonds, New J. Phys. **10**, 115001 (2008).
[18] K. Jähne, C. Genes, K. Hammerer, M. Wallquist, E. S. Polzik, and P. Zoller, Phys. Rev. A **79**, 063819 (2009).
[19] K. Stannigel, P. Rabl, A. S. Sørensen, M. D. Lukin, and P. Zoller, Phys. Rev. A **84**, 042341 (2011).
[20] Y.-D. Wang and A. A. Clerk, Phys. Rev. Lett. **110**, 253601 (2013).
[21] J.-Q. Liao, Q.-Q. Wu, and F. Nori, Phys. Rev. A **89**, 014302 (2014).
[22] H. J. R. Westra, M. Poot, H. S. J. van der Zant, and W. J. Venstra, Phys. Rev. Lett. **105**, 117205 (2010).
[23] K. J. Lulla, R. B. Cousins, A. Venkatesan, M. J. Patton, A. D. Armour, C. J. Mellor, and J. R. Owers-Bradley, New J. Phys. **14**, 113040 (2012).

[24] R. Khan, F. Massel, and T. T. Heikkilä, Phys. Rev. B **87**, 235406 (2013).
[25] H. Yamaguchi and I. Mahboob, New J. Phys. **15**, 015023 (2013).
[26] A. A. Clerk, F. Marquardt, and K. Jacobs, New J. Phys. **10**, 095010 (2008).
[27] J.-Q. Liao and C. K. Law, Phys. Rev. A **83**, 033820 (2011).
[28] T. A. Palomaki, J. W. Harlow, J. D. Teufel, R. W. Simmonds, and K. W. Lehnert, Nature (London) **495**, 210 (2013).
[29] T. A. Palomaki, J. D. Teufel, R. W. Simmonds, and K. W. Lehnert, Science **342**, 710 (2013).
[30] M.-A. Lemonde, N. Didier, and A. A. Clerk, Phys. Rev. Lett. **111**, 053602 (2013).
[31] J. Qian, A. A. Clerk, K. Hammerer, and F. Marquardt, Phys. Rev. Lett. **109**, 253601 (2012).
[32] P. D. Nation, Phys. Rev. A **88**, 053828 (2013).
[33] N. Lörch, J. Qian, A. Clerk, F. Marquardt, and K. Hammerer, Phys. Rev. X **4**, 011015 (2014).
[34] S. Rips, M. Kiffner, I. Wilson-Rae, and M. J. Hartmann, New J. Phys. **14**, 023042 (2012).
[35] L. Tian, Phys. Rev. B **72**, 195411 (2005).
[36] A. Voje, J. M. Kinaret, and A. Isacsson, Phys. Rev. B **85**, 205415 (2012).
[37] F. Xue, Y.-x. Liu, C. P. Sun, and F. Nori, Phys. Rev. B **76**, 064305 (2007).
[38] G. Z. Cohen and M. Di Ventra, Phys. Rev. B **87**, 014513 (2013).
[39] H. Tan, G. Li, and P. Meystre, Phys. Rev. A **87**, 033829 (2013).
[40] X.-W. Xu, Y.-J. Zhao, and Y.-x. Liu, Phys. Rev. A **88**, 022325 (2013).
[41] J. Suh, M. D. LaHaye, P. M. Echternach, K. C. Schwab, and M. L. Roukes, Nano Lett. **10**, 3990 (2010).
[42] F. Massel, T. T. Heikkila, J.-M. Pirkkalainen, S. U. Cho, H. Saloniemi, P. J. Hakonen, and M. A. Sillanpaa, Nature (London) **480**, 351 (2011).
[43] A. Eichler, J. Moser, J. Chaste, M. Zdrojek, I. Wilson-Rae, and A. Bachtold, Nat. Nano **6**, 339 (2011).
[44] A. Voje, A. Isacsson, and A. Croy, Phys. Rev. A **88**, 022309 (2013).
[45] K. Jacobs, arXiv:1209.2499.
[46] I. Mahboob, K. Nishiguchi, A. Fujiwara, and H. Yamaguchi, Phys. Rev. Lett. **110**, 127202 (2013).
[47] K. V. Kheruntsyan and K. G. Petrosyan, Phys. Rev. A **62**, 015801 (2000).
[48] K. J. McNeil and C. W. Gardiner, Phys. Rev. A **28**, 1560 (1983).
[49] W. J. Munro, Phys. Rev. A **59**, 4197 (1999).
[50] M. D. Reid and L. Krippner, Phys. Rev. A **47**, 552 (1993).
[51] H. M. Wiseman and G. J. Milburn, Phys. Rev. A **47**, 642 (1993).
[52] M. D. Reid and P. D. Drummond, Phys. Rev. Lett. **60**, 2731 (1988).
[53] P. Marian, T. A. Marian, and H. Scutaru, Phys. Rev. A **68**, 062309 (2003).
[54] A. Gilchrist, P. Deuar, and M. D. Reid, Phys. Rev. Lett. **80**, 3169 (1998).
[55] G. Adesso and F. Illuminati, J. Phys. A: Math. Theor. **40**, 7821 (2007).
[56] J. M. Fink, M. Göppl, M. Baur, R. Bianchetti, P. J. Leek, A. Blais, and A. Wallraff, Nature (London) **454**, 315 (2008).
[57] I. Schuster, A. Kubanek, A. Fuhrmanek, T. Puppe, P. W. H. Pinkse, K. Murr, and G. Rempe, Nat. Phys. **4**, 382 (2008).
[58] A. Miranowicz, M. Bartkowiak, X. Wang, Y.-x. Liu, and F. Nori, Phys. Rev. A **82**, 013824 (2010).
[59] R. Simon, Phys. Rev. Lett. **84**, 2726 (2000).
[60] L.-M. Duan, G. Giedke, J. I. Cirac, and P. Zoller, Phys. Rev. Lett. **84**, 2722 (2000).
[61] N. Brunner, D. Cavalcanti, S. Pironio, V. Scarani, and S. Wehner, Rev. Mod. Phys. **86**, 419 (2014).
[62] E. G. Cavalcanti, C. J. Foster, M. D. Reid, and P. D. Drummond, Phys. Rev. Lett. **99**, 210405 (2007).
[63] J. Wenger, M. Hafezi, F. Grosshans, R. Tualle-Brouri, and P. Grangier, Phys. Rev. A **67**, 012105 (2003).
[64] J. F. Clauser and M. A. Horne, Phys. Rev. D **10**, 526 (1974).
[65] J. F. Clauser, M. A. Horne, A. Shimony, and R. A. Holt, Phys. Rev. Lett. **23**, 880 (1969).
[66] M. Grajcar, S. Ashhab, J. R. Johansson, and F. Nori, Phys. Rev. B **78**, 035406 (2008).
[67] S. Sapmaz, Y. M. Blanter, L. Gurevich, and H. S. J. van der Zant, Phys. Rev. B **67**, 235414 (2003).
[68] A. M. Eriksson, D. Midtvedt, A. Croy, and A. Isacsson, Nanotechnology **24**, 395702 (2013).
[69] A. Castellanos-Gomez, H. B. Meerwaldt, W. J. Venstra, H. S. J. van der Zant, and G. A. Steele, Phys. Rev. B **86**, 041402 (2012).
[70] K. Jacobs and A. J. Landahl, Phys. Rev. Lett. **103**, 067201 (2009).
[71] M. J. Woolley, G. J. Milburn, and C. M. Caves, New J. Phys. **10**, 125018 (2008).
[72] I. Mahboob, K. Nishiguchi, H. Okamoto, and H. Yamaguchi, Nat. Phys. **8**, 387 (2012).
[73] Y. Okazaki, I. Mahboob, K. Onomitsu, S. Sasaki, and H. Yamaguchi, Appl. Phys. Lett. **103**, 192105 (2013).
[74] M. Paternostro, D. Vitali, S. Gigan, M. S. Kim, C. Brukner, J. Eisert, and M. Aspelmeyer, Phys. Rev. Lett. **99**, 250401 (2007).
[75] A. A. Clerk, M. H. Devoret, S. M. Girvin, F. Marquardt, and R. J. Schoelkopf, Rev. Mod. Phys. **82**, 1155 (2010).
[76] C. Eichler, D. Bozyigit, C. Lang, M. Baur, L. Steffen, J. M. Fink, S. Filipp, and A. Wallraff, Phys. Rev. Lett. **107**, 113601 (2011).
[77] N. Bergeal, F. Schackert, L. Frunzio, and M. H. Devoret, Phys. Rev. Lett. **108**, 123902 (2012).
[78] F. Mallet, M. A. Castellanos-Beltran, H. S. Ku, S. Glancy, E. Knill, K. D. Irwin, G. C. Hilton, L. R. Vale, and K. W. Lehnert, Phys. Rev. Lett. **106**, 220502 (2011).
[79] E. Flurin, N. Roch, F. Mallet, M. H. Devoret, and B. Huard, Phys. Rev. Lett. **109**, 183901 (2012).
[80] M. Ludwig, A. H. Safavi-Naeini, O. Painter, and F. Marquardt, Phys. Rev. Lett. **109**, 063601 (2012).
[81] I. S. Grudinin, H. Lee, O. Painter, and K. J. Vahala, Phys. Rev. Lett. **104**, 083901 (2010).
[82] G. Bahl, J. Zehnpfennig, M. Tomes, and T. Carmon, Nat. Commun. **2**, 403 (2011).
[83] J. R. Johansson, P. D. Nation, and F. Nori, Comp. Phys. Commun. **183**, 1760 (2012).
[84] J. R. Johansson, P. D. Nation, and F. Nori, Comp. Phys. Commun. **184**, 1234 (2013).
[85] The source code for the numerical simulations is available on Figshare, http://dx.doi.org/10.6084/m9.figshare.936910.